Water and Soil Management and Modeling

Online ISSN: 2783 - 2546

University of Mohaghegh Ardabili

Synergistic effect of land use and climate change on evapotranspiration

Damte Tegegne Fetene [1], Tarun Kumar Lohani [2*], Abdella Kemal Mohammed [3]

[1] Ph.D. scholar of Hydraulic Engineering, Faculty of Hydraulic & Water resources Engineering, Arba Minch University, Arba Minch, Ethiopia

[2] Professor, Faculty of Hydraulic & Water resources Engineering, Arba Minch University, Arba Minch, Ethiopia

[3] Associate Professor, Faculty of Hydraulic & Water resources Engineering, Arba Minch University, Arba Minch, Ethiopia

Abstract

Evapotranspiration (ET) is the second most important element of the hydrological cycle after rainfall. Despite rising attention in hydrological responses to environmental change, limited extensive evaluations of AET have been conducted in the study watershed that integrates the combined influences of LULC and climate change. Previous research has largely focused on broader areas, such as the LTSB and the Abbay Basin, offering a limited understanding of localized relations between these factors. Therefore, this study investigates the synergistic impacts of LULC dynamics and climate change on AET within the Guna Tana Watershed (GTW) using the physically based MIKE SHE hydrological model, aiming to improve understanding of watershed-scale hydrological responses under future environmental conditions. ENVI 5.3 and QGIS 2.18.15 were used to assess the LULC classification and prediction, respectively. Ensembles of GCM were used after bias correction, and calibration of the model was done using streamflow. Agriculture was expanded from 2047.02 km^2 to 2268.82 km^2, whereas forest will decline to 103.38 km^2 from 127.64 km^2 in the 1991-2021 period. Built-up showed the least amount of coverage (0.02%, 0.11%, and 0.31%). The results of the calibration and validation show that MIKE SHE is capable of modeling the AET effectively. Excellent results were indicated in two watersheds by both calibration and validation (R =0.87-0.94). The rise in AET may be detrimental to the watersheds because it reduces streamflow and groundwater recharge. Moreover, soil moisture stress increases the risk of drought. Projected changes in AET relative to the baseline period indicate increasing trends in both the Gumara and Ribb watersheds under future climate scenarios. In the Gumara watershed, mean annual AET is expected to rise moderately, with increases of 3.25% and 1.19% in the 2020s and 2050s under SSP2-4.5, and 5.09% and 8.01% under SSP5-8.5. The Ribb watershed shows a stronger response, with AET increasing by 16.92% and 19.30% under SSP2-4.5, and 14.13% and 22.07% under SSP5-8.5. All of this presents problems for the environment and water balance downstream, such as Lake Tana. Future research should include additional climate models and ground truth data regarding plant characteristics to increase model accuracy and reduce uncertainty.

Keywords: AET, ENVI, Land use change, MIKE SHE, QGIS

Article Type: Research Article

Academic Editor: Raoof Mostafazadeh

*Corresponding Author, E-mail: tklohani@gmail.com

Citation: Fetene, D.T., Lohani, T.K., & Mohammed, A.K. (2026). Synergistic effect of land use and climate change on evapotranspiration. Water and Soil Management and Modeling, 6 (Special Issue: New Approaches to Water and Soil Management and Modeling), 121-139.

doi: 10.22098/mmws.2025.18634.1710

Received: 26 October 2025, Received in revised form: 15 November 2025, Accepted: 24 November 2025, Published online: 03 June 2026

Water and Soil Management and Modeling, Year 2026, Vol. 6, Special Issue, pp. 121-139.

Publisher: University of Mohaghegh Ardabili

© Author(s)

1. Introduction

Terrestrial ET, the second most imperative component of the water cycle after rainfall, has been well documented around the globe. It absorbs around 60% of the energy, returns approximately 70% of the precipitation, and contributes a total water loss of nearly 50% (Ji et al., 2024; Ma & Szilagyi, 2019). ET is an indispensable feature for the energy budget of atmospheric systems. Adequate water and higher agricultural output levels are required for the increasing global population (Sinha et al., 2021). For this reason, developing effective regional management devices needs precise measurement of ET (Ghaderi et al., 2020). However, the direct measurement is complex (Nunno & Granata, 2023), and the estimation of all water balance components, especially ET, is necessary for meticulous irrigation planning (Granata, 2019).

For crop and water management, the valuation of AET is a basic task (Senay et al., 2020). It is pivotal to quantify AET in natural vegetation to assess the water status of ecosystems and water use in basins (Awada et al., 2021). A precise estimate of AET and determining its major influences is decisive (Cao et al., 2023). Nevertheless, the ET is affected by changes in LULC and climate (Omondi et al., 2019). The altering characteristics of AET, which accounts for nearly 59% of global precipitation, and its impacts are at the forefront of climate variation studies (Hong et al., 2023).

An issue facing planners and managers of water resources is the future availability and demand for clean water. This irresolution is being exacerbated by changes in LULC and climate, which are probably to modify the frequency of HPs (Kuma et al., 2021). For effective WRM, land use planning, and sustainable development, it is essential to comprehend the hydrological responses to past and projected LULC change (Ayalew et al., 2024). Understanding the tweaking in land use influence on ET is a herculean task (Zheng et al., 2020). Recently, LULCC-induced ET alterations have been focused on with specific interest (Qilin et al., 2021). In arid and semi-arid regions, accurate ET estimation is vital for managing water use, irrigation, and droughts (Abbasi et al., 2021). Nonetheless, there is conflict among the LTSB water users, particularly concerning agricultural output (Taye et al., 2021). This is why sub-basins need to measure the LULC and climatic impact on AET.

GCMs are applied to exemplify the present and future changes in climate. Since 2013, the CMIP has continued to release new datasets. CMIP6, compared with CMIP5, offers datasets with higher spatial resolution and more advanced algorithms, improving the accuracy of climate projections (Seifu & Eshetu, 2024). To predict future climatic variables, GCMs play a vital role, but the spatial resolution is a matter of concern. As a result, the raw outputs of GCM become inappropriate for catchment and indecisive regional-scale studies (Deb et al., 2018). GCM outputs are fully biased and are seldom used directly. Systematic errors, coarse spatial resolution, and simplified physics and thermodynamics are sources of biases in the simulations of climate models (Das et al., 2020). However, the problem can be solved by BC, which is desirable to minimize the error (Chen et al., 2018). Quintile mapping (QM) has been employed in bias-corrected projection for the GCMs (Afzal & Ragab, 2020). In climate alteration influence studies, an ensemble of GCM outputs is often used to illustrate a reasonable range for upcoming climate conditions (Seo et al., 2019).

HM models (HM) are usually used to estimate the areal AET next to calibration using observed discharge (Birhanu & Kim, 2019). Some of the HPs in a watershed that are mostly modeled by the HM are groundwater and stream discharge, infiltration, and ET (Adjei et al., 2023). Many ET studies using HM have been undertaken around the globe (Ahn et al., 2018; Chen et al., 2024; Marek et al., 2016) using the SWAT model, CLIME-MG (Gisolo et al., 2022), and VIC to estimate AET (Gao et al., 2020). In Ethiopia, some of the research has been done in, Melka Kuntre watershed (Mekonnen et al., 2021), Bilate River Basin (Nannawo et al., 2022), Bebeks and Shina area in LTSB using the Hydrus model (Beyene et al., 2018). However, in the LTSB, ET has not been given much privilege. In recent years, several researchers have contributed to using MIKE SHE HM, which is an advanced and adaptable framework (Wang et al., 2023).

The relation between surface ET and climate warming is complex; consequently, resolving this issue could increase the understanding of the terrestrial water cycle (Zhang et al., 2019). The world's warming is observed due to climate change, and this will raise AET, further depleting the planet's finite water supplies (Ajjur et al., 2021; Kundu et al., 2018; Hyandye et al.,2018). AET is an essential element of the global water and energy system (Yang et al., 2020) and has a substantial effect on regional climate characteristics (Peng et al., 2019; Xiong et al., 2019). Reliable estimations of AET are beneficial for sustainable WRM, including irrigation planning, drought assessment, and predicting the demand for water in vast farmland (Demirel et al., 2018). Understanding human activity and climate change implications on energy and water fluxes in ecosystems is decisive. Research on ET's response to LUCC and climate tweaking is also indispensable (Hejia et al., 2019).

The shifting patterns of land use brought about by the growth of agricultural land require a crucial observation in Ethiopia (Dufera & Brijesh, 2023). LULC changes are a major environmental concern in Ethiopia, where agriculture is the key pillar of the economy. Previous studies have documented considerable changes in LULC across the country since the late 20th century (Liyew et al., 2019). Understanding climate variability and how it affects hydrological elements requires a thorough analysis of how it affects ET (Yang et al., 2017). Accurate data on every element of the hydrological cycle is necessary to effectively manage water resources (Rahim et al., 2012). However, in many areas of Ethiopia, there are not enough meteorological stations to estimate geographically suitable reference ET, and the absence of spatial heterogeneity in crop coefficient is a glaring obstacle to effective irrigation water management (Mebrie et al., 2023). Because of this, estimating ET is valuable for water yield, water resources, and ecosystem services management. According to Abebe et al. (2022), ET constitutes about 58% of water loss in the Abay basin. Conversely, Mohamed et al. (2025) reported that AET represents 40%.

The Abay Basin is regarded as one of Ethiopia's major basins (Worqlul et al., 2018). Ethiopia's government designated the LTSB as a growth corridor (Kindie et al., 2019). Furthermore, the LTSB is a source of the Abay basin and is regarded as the main economic zone because of its considerable capability for tourism, agriculture, and additional economic activity (Getachew & Manjunatha, 2021). Exploring and comprehending the variability in AET is challenging, and the multifaceted connections among terrestrial storage, vegetation, climate, and human activity cause temporal variability in AET (Wu et al., 2017). The AET under the influence of both climate and land use has not been studied yet in GTW. This study's primary objective was to assess how land use and climatic variation affect AET in GTW using MIKE SHE. The use of MIKE SHE in conjunction with LULC and CMIP6 data shows a robust scientific methodology (Farjad et al, 2017). The research gains depth when hydrological modeling and climatic projections are combined. In the future, Surface water balancing, project management, and irrigation water management in GTW will all benefit from a scientific understanding of how LULC and climate change affect AET.

In the study watershed, there has been no detailed assessment of AET that considers the combined effects of LULC change and climate change. Most previous studies have focused on larger areas, such as the Lake Tana Sub-Basin (LTSB) or the Abbay Basin, leaving a limited understanding of how these two factors interact to influence AET at the local watershed scale. Therefore, this study investigates the Synergistic impact of LULC and climate change in GTW.

2. Materials and Methods

2.1 Study area

GTW is found in Ethiopia, South Gondar, with the Gumara and Ribb rivers starting from the Guna Mountain and flowing westward (Mulatu et al., 2021). The watershed is located in ‘‘37° 30 ′to 38° 10 ′east and 11° 30 to 12° 20 ′north’. The gauged area of the GTW is 2597.11 km^2, but the entire area of the GTW is 3548.4 km^2 (Figure 1) and (Fetene et al., 2023). Only the upper part of the rivers is gauged (Alemu et al., 2020), and every modeling process was carried out in the gauged area. The GTW climate is experiencing the tropical highland monsoon (Berhanu et al., 2024). The highest point of the GTW is Guna Mountain, 4100 m above sea level (Teressa et al., 2021).

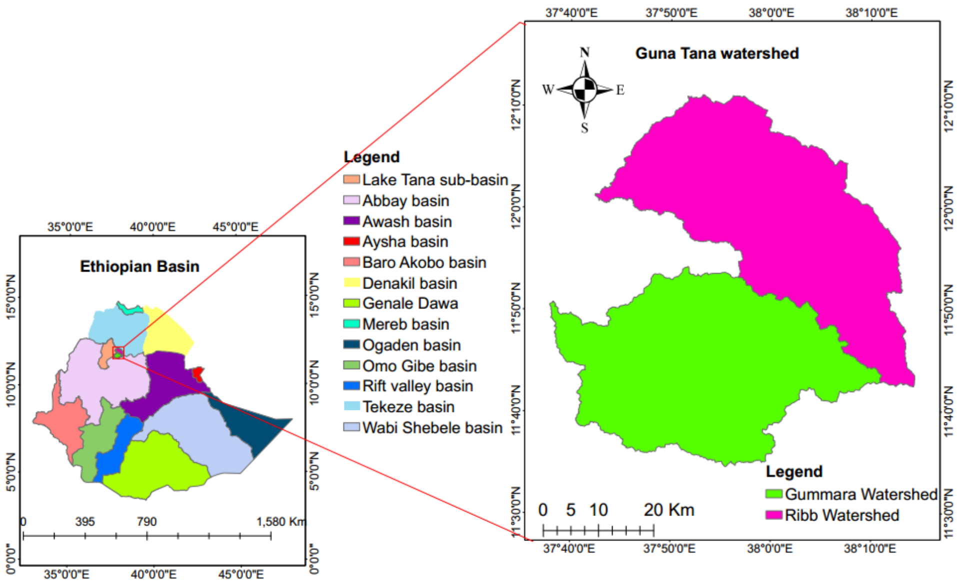

Figure 1. Study area map

2.1. Hydro-Meteorological data

The National Meteorological Institute (NMI) provided the meteorological data from 1985-2014, including rainfall, temperature, sunshine hours, relative humidity, and wind speed for three stations. For the others, only temperature and rainfall were gained. Ministry of Water and Energy (MoWE) and Abay Basin Authority provided streamflow data for the Gumara and Ribb gauge stations. GCPs were collected during field visits, and GCM data were downloaded from the WCRP (World Climate Research Program) CMIP6 archive[1](Kim,2024), with the baseline period was 1985-2014 and the future period of 2016-2075. Systematic biases significantly contribute to the inaccuracies observed in climate forecasts, highlighting the necessity of applying bias correction (BC) methods (Yuning et al., 2025). BC was done for the downloaded GCM in the climate model data for hydrological modelling (CMhyd) using QM. Due to its strong capability to adjust the cumulative results from climate models distributed to correspond with observed data, QM has become a commonly applied BC method (Wu et al., 2023).

Before being used as input for the model, the homogeneity of the mean annual rainfall data was examined using the Pettit and Standard Normal Homogeneity test (SNHT) at the 95 percent confidence level. All of the records were homogeneous, according to the results.

2.2. Remote sensing data

Landsat images of level 1 for the years 1991, 2007, and 2021 were acquired from the USGS Earth Resources Observation and Science Center via the Earth Explorer platform[2] (Lanfredi et al., 2022) during clear skies to minimize cloud interference and improve image quality. The DEM data were downloaded from Alaska [3]. Satellite remote sensing data were processed in ENVI software to produce detailed LULC maps of GTW. Soil types for the watersheds were downloaded from the Food and Agriculture Organization[4].

2.3. Accuracy assessment and confusion matrix

Finding the reliability of a LULC mapping is a crucial step. The quality of the satellite-based LULC mapping is largely determined by the

[1] https://esgf-node.llnl.gov/search/cmip6
[2] https://earthexplorer.usgs.gov
[3] https://asf.alaska.edu/data-sets/sardatasets/alos-palsar
[4] https://www.fao.org/soils-portal

accuracy (Al-Dousari et al., 2023). The predicted overall accuracy and Kappa index have been used to evaluate the categorization correctness of satellite images.

To evaluate accuracy, a post-classification and confusion matrix were performed. The matrix was used to analyze changes in land usage over a certain time frame. According to land use data in 1991, 2007, and 2021, the area of different land types and confusion matrices (1991–2007, 2007–2021, and 1991–2021) (Wu et al., 2024). It is feasible to illustrate the shifting features of the land use matrix to describe the conversion relationship between land use categories during different periods in the GTW, as well as the direction of reciprocal transfer. This will reflect the trend of land use type transfer (Li et al., 2024).

$$\mathrm{Sij} = \begin{bmatrix} S_{11} & S_{12} & \cdots & S_{1g} \\ S_{21} & S_{22} & \cdots & S_{2g} \\ \vdots & \vdots & \cdots & \vdots \\ S_{k1} & S_{k2} & \cdots & S_{ka} \end{bmatrix} \quad (1)$$

Where Sij denotes the land use status, and k and g are different land use categories.

2.4. Image classification and prediction

To classify the LULC, supervised classification using a support vector Machine (SVM) has been used. SVM is an effective technique for image classification since it requires fewer samples and is less prone to correlated bands than the maximum likelihood (MLC) (Amare et al., 2023). Using the layer stack feature in the ENVI 5.3 software, the satellite images were layered into a single layer. The software ENVI 5.3 was used to preprocess Landsat images for atmospheric correction, layer stacking, and mosaicking. The Landsat ETM+ image stripping lines were removed with QGIS using image enhancement algorithms. After mapping and measuring accuracy for 1991, 2007, and 2021, LULC was predicted for 2035 and 2049 by using QGIS 2.18.15. Cellular automata (CA) investigate local LULC circumstances using recent LULC data rather than a variety of historical data (Soumya & Neeta, 2023). Using a CA-ANN (artificial neural network) model, the future LULC has been examined (Rahman & Rahman, 2023). QGIS plugin MOLUSCE was used to forecast and fix potential LULC change for 2035, 2049 (Amgoth et al., 2023).

2.5. The CMIP6 model and bias correction

The four socioeconomic factors influencing the Shared Socioeconomic Pathways (SSPs) are population, education, urbanization, and economic development. CMIP6 offers climate model projections reflecting various socioeconomic pathways and climate change impacts. The possible outcomes indicated that, if the maximum emission scenario is implemented, the temperature would rise by 1.5°C in 2021–2040 and 3.3–5.7 °C in the long future 2081–2100 (Siabi et al., 2023). Using an ensemble of seven models, the AET under the impact of anthropogenic and climate variability in the GTW was estimated under SSP2-4.5 and SSP5-8.5 between 2016 and 2075 (Fetene et al., 2024). The GCM forecasts were made employing an ensemble of models in order to minimize uncertainty (Gholami et al., 2023), and the GCM models were selected based on their performance. Additionally, the seven CMIP models were selected based on the accessibility of data for both historical and forthcoming periods on the SSP2-4.5 and SSP5-8.5 in r1i1p1f1 labels. SSP2-45 and 5-85 were chosen because they are scenarios with medium and high emissions, whereas SSP1-1.9 and SSP1-2.6 are less susceptible (Shiru et al., 2022).

The models were bias-corrected before being applied to climate variability impact assessment. BC is essential for improving the accuracy of CMIP6 model simulations and has important ramifications for disaster risk reduction, WRM, and climate influence analyses (Addisuu et al., 2025). BC is an important step in using Earth systems model outputs for evaluations, adjusting systematic errors by comparing them to observations (Ganguli et al., 2025).

2.6. Hydrological Model Setup

The AET change process can be accurately replicated using the hydrological modeling, which also distinguishes between the effects of land use and climate dynamics on the HPs. It is unable to fully investigate how Land use dynamics affect the AET change, though (Lu et al., 2024). To guesstimate the current and future AET changes in the GTW MIKE SHE software was used. In accordance with the supplied data's accessibility, the MIKE SHE operational structure's flexibility permits the employment of any number of water cycle components (Rahim & Yusoff, 2023). The MIKE SHE model evaluates ET, surface flow, unsaturated flow, saturated flow, subsurface flow, and channel flow (Werede et al., 2024) as well as their interconnections (Li et al., 2022).

MIKE SHE simulates AET based on empirical parameters, Leaf Area Index, and rooting depth for each species of vegetation using the Kristensen-Jensen technique (Sharma et al., 2024) and a two-layer water balance method. In the MIKE SHE model, the ET rate, the vegetation properties, and the soil moisture can be calculated. In MIKE SHE, the 2-layer water balancing approach has been used to model the AET using Equation 2 (Patel, 2018; Shing et al., 2021).

$$AET = E_c + E_p + E_u + E_s \qquad (2)$$

Ec is evaporation from canopy storage, Ep is evaporation from soil, Eu is the daily ET amount from the unsaturated zone, and Es is the daily ET from the saturated zone.

2.7. Calibration of the hydrological model

Regarding HM's response to historical and observed data to be matched, the model's parameter values need to be calibrated. Typically, a small number of stations' worth of observed and simulated runoff are compared to calibrate the model (Pan et al., 2018). A completely distributed model with several components is difficult to calibrate; thus, for the calibration process, only a small number of sensitive factors were selected. These settings were determined through manual sensitivity analysis (SA) (Vu et al., 2017). Since SV is important for lessening and evaluating uncertainty in computer-based models (Duan et al., 2019). In the MIKE SHE model, Mannings_M, RD, LAI, and crop coefficient (Kc) are pivotal parameters for AET. To evaluate the accuracy between simulated and observed discharge, the Nash-Sutcliffe efficiency (NSE) index has been developed (Lee et al., 2018). Figure 2 shows the overall workflow for this investigation.

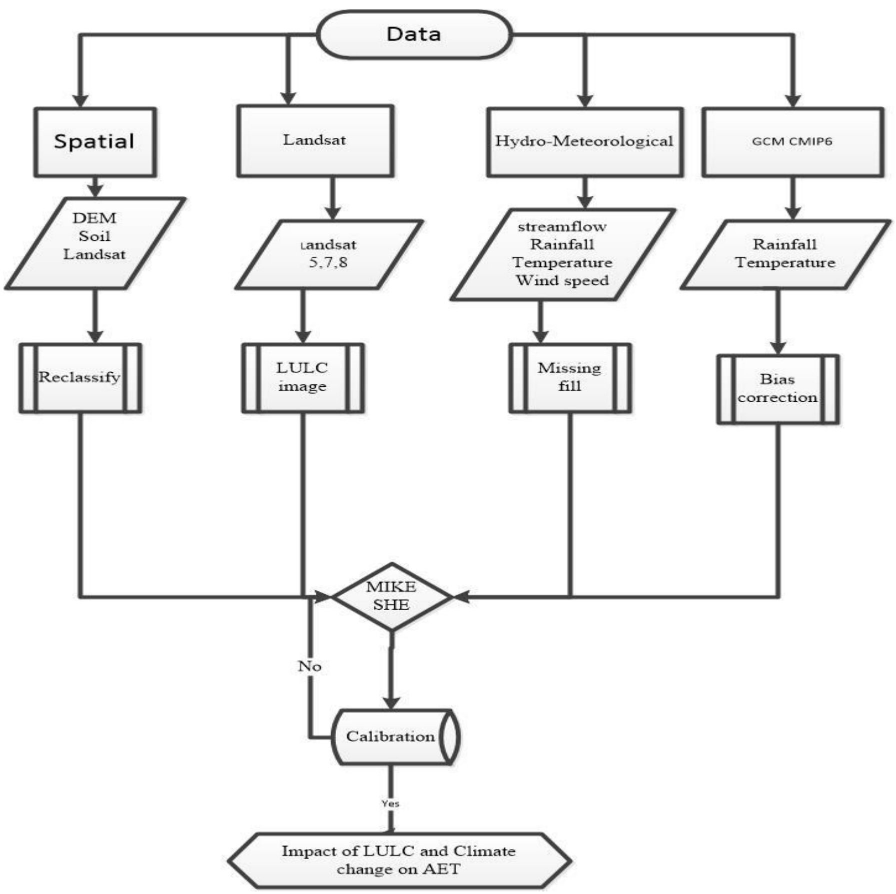

Figure 2. Flowchart of methodological processes

+3. Results and Discussion

3.1. LULC classification and assessment of accuracy

LULC is a compulsory input for the majority of analysis and prediction activities; it is a critical spatial data source (Puttinaovarat et al., 2025). Since LULC categorization is one of the key subjects in remote sensing, accurate information on a region's LULC change is necessary for any country to plan and manage its resources effectively (Tarafdar et al., 2025). Built-up, shrubland, water body, farmland, grassland, forest, and bareland were the land use types used to categorize the downloaded Landsat pictures of the GTW for the years 1991, 2007, and 2021. In 1991, 2007, and 2021, agriculture accounted for 78.82%, 82.81%, and 87.34% of the watershed area, respectively (Table 1). The minimal area coverage was perceived by built-up (0.02%, 0.11%, and 0.31%), surpassed by water bodies (0.12%, 0.17%, and 0.6%) in 1991, 2007, and 2021, respectively.

Table 1. Land use class of GTW

	1991		2007		2021	
	Area (km^2)	Area (%)	Area (km^2)	Area (%)	Area (km^2)	Area (%)
Built-up	0.51	0.02	2.82	0.11	8.08	0.31
Forest	127.64	4.91	95.18	3.66	103.38	3.98
Water	3.18	0.12	4.42	0.17	15.61	0.60
Agriculture	2047.02	78.82	2150.56	82.81	2268.33	87.34
Grassland	180.96	6.97	127.38	4.90	95.65	3.68
Shrubland	153.72	5.92	123.58	4.76	70.38	2.71
Bare Land	84.17	3.24	93.17	3.59	35.69	1.37
Total	2597.11	100.00	2597.11	100.00	2597.11	100.00

Maintaining map accuracy is essential since a map is incomplete without a thorough understanding of its accuracy. An accuracy range of 85 to 90% is typically regarded as the norm for accurately classifying various land cover categories (Doost & Yaseen, 2025). The error matrix was created by acquiring GCP data from the field and Google Earth Pro in ArcGIS software. Elder community interviews were also utilized. Kappa statistics, user accuracy, producer accuracy, and total accuracy were used to assess the model's performance. The producer accuracy ranged from 0.73 to 0.95. The kappa statistics for GTW were 0.81, 0.86, and 0.9 in 1991, 2007, and 2021, respectively. Accurate LULC data are critical for monitoring land use alteration driven by environmental and human interaction. LULC change studies are important for tracking SGDS and climate impact.

3.2. Change detection and prediction

The built-up, agricultural, and water bodies show a gradual progression during the previous three decades. In 1991-2007, the built-up up noticed a 452.94% increase in percentage, but the forest decreased by 25.43% (Table 2). The outcomes of this study indicate that between 2007 and 2021 built-up area upsurge by 186.52%, agricultural land by 5.48%, and forest by 8.62%, while the area of the shrubland decreased by 43.05%. Grasslands and shrublands show declining conditions (Table 2). The trends for forest land were inconsistent, declining from 1991 to 2007 and then rising from 2007 to 2021. A minor increase in forestland was observed in the watershed over the period 2007-2021. This change may be basically due to the increase in eucalyptus plantations as an income for the community (Moges & Bhat, 2017) in the upstream of the GTW. A comparable mode is witnessed in Guna Mountain, the upper part of the watersheds (Belay et al., 2022). The construction of an artificial reservoir such as Ribb Dam, which spans 9.78 km^2, could be the cause of the water body area's startling expansion in 2021 (Alebachew et al., 2022).

The projection of LULC is subject to the uncertainty of factors, including population growth, economic expansion, and policy changes. Furthermore, sources of uncertainty include model uncertainty and data error, like noise and resolution in remote sensing (Chen et al., 2022). However, by utilizing the machine learning classifier SVM for classification and CA-ANN for prediction, in addition to the accuracy evaluation, the uncertainty was decreased.

Table 1. Detection of changes in land use

Land use classes	% Change during 1991-2007	% Change during 2007-2021	% Change during 1991-2021
Built-up	452.94	186.52	1484.31
Forest	-25.43	8.62	-19.01
Water	38.99	253.17	390.88
Agriculture	5.06	5.48	10.81
Grassland	-29.61	-24.91	-47.14
Shrubland	-19.61	-43.05	-54.22
Bare Land	10.69	-61.69	-57.60

The future land uses were predicted by QGIS 2.18.15 using the MOLUSCE plugin for 2035 and 2049 years. Agriculture and water bodies increased dramatically in both watersheds, whereas grassland and shrubland decreased. Comparing 2035 to 2049 land use, bare land, built-up, agriculture, and forest indicate incremental trends, while the shrubland and grassland indicate a reduction trend.

3.3. Calibration and Validation

Many calibration parameters for the MIKE SHE are available depending on the module being used. By running the model with a changing parameter value and assuming that the other parameters remain constant, the most sensitive parameter was examined. The time constants for base flow and interflow, as well as RD, LAI, and Mannings_M, were the most important parameters. Streamflow is affected by changes in Mannings_M; higher Mannings_M results in lower discharge, and vice versa. AET is impacted by LAI; a rise in LAI may raise AET, while a decrease in LAI may lower AET. The calibration was verified using monthly-observed discharge data from the Gumara and the Ribb River. The model was used for 7 years of validation (30% of the data) (2000–2007) and 15 years of calibration (70% of the discharge data) (1985–1999).

The initial parameter values for the MIKE SHE calibration/ validation were obtained from earlier research and the MIKE SHE user manual. Table 3 displays the simulated and actual flow for the calibration/validation results. The simulation has rationally captured the observed flow. Both R and NSE indicated excellent results in two watersheds. R was always higher than 0.9 during the calibration-validation phase, except for the Ribb watershed calibration phase, when R was 0.87. In addition to the Ribb watershed calibration, the NSE value exceeded 0.8. The correlation was done monthly basis.

Table 3. Calibration validation result of watersheds

Statistics	Gumara watershed		Ribb watershed	
	calibration	validation	calibration	validation
NSE	0.804	0.84	0.75	0.88
R	0.90	0.91	0.87	0.94
RMSE	676.38	656.94	371.07	250.62

3.4 Projected Changes in Temperature and Rainfall

Many researchers have proposed a multi-model ensemble to reduce single-model uncertainty (Shen et al., 2018). The mean monthly future temperature was compared with the baseline after QM-based BC. The temperature might increase in both periods relative to baseline periods (Figure 3a). This outcome is witnessed by Wubneh et al. (2024) in the LTSB using an RCP 4.5 and 8.5. The increment in minimum temperature is greater in all months relative to maximum temperature. This rise in future temperature is also indicated by Tikuye et al. (2024) in LTSB, which might rise to 4.6 °C. However, GTW will increase to 2.9 °C and 4.6 °C in SSP2-4.5. The research area's increasing ET rate due to rising temperatures throughout the dry season resulted in water shortages, and this problem is expected to get worse (Ferede et al., 2022). According to Figures 3a and b, the temperature will be beyond the Paris Agreement

Article 2a, the temperature increase is limited to 2°C until 2050 (Savaresi, 2016).

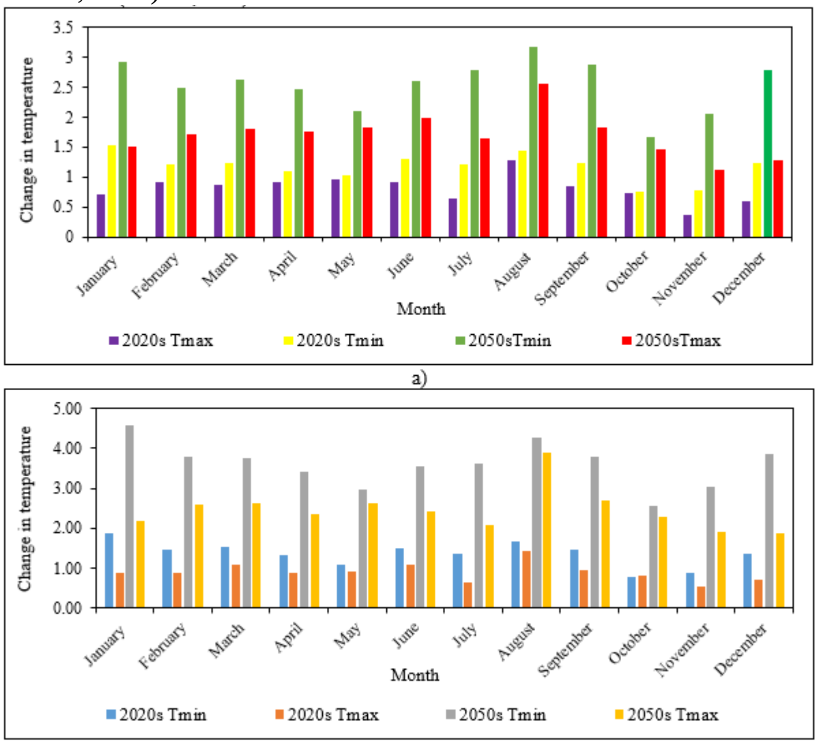

a)

b)

Figure 3. Temperature Change in a) SSP2-4.5 and b) SSP5-8.5

The average monthly rainfall in most months will decrease, but in September- November, the rainfall is likely to increase (Figure 4). In December, February, and March, there might be a maximum decrease in rainfall, particularly in the 2050s at SSP5-8.5. The percentage alteration in precipitation was not regular, i.e., precipitation rises in some months and declines in other months in the Megech watershed, similar to the study watersheds (Addisu et al., 2024). According to earlier research conducted in the Abay basin, rainfall may have decreased by as much as 50% (Bekele et al., 2019). In the research area, rainfall increases after the major rainy season (September-November). This result shows how the model's output is comparable to previous studies. The findings were similar in Gilgel Abay watersheds by Abdo et al. (2009). This variability in the rainy season can affect farming activities and crop production.

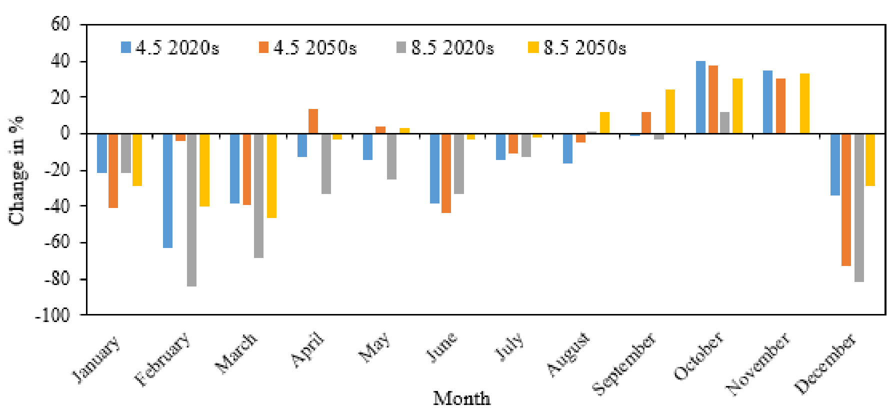

Figure 1. Change in mean monthly rainfall relative to baseline

3.5. LULC and climate change on monthly changes of AET

AET response to both LULC and climate alteration across two periods (2016–2045 and 2046–2075) using SSP2-4.5 and SSP5–8.5 was appraised in the GTW. The LULC maps of 2035 and 2049 represented the 2020s and 2050s, respectively. Regarding the baseline result, the influence was compared at the monthly, seasonal, and yearly levels. However, the simulation was done daily in the MIKE SHE model and accumulated over months and above. In both watersheds during wet months, the monthly AET might be maximum in all scenarios compared to the baseline (Figure 5). The lowest monthly AET might be observed in dry periods, particularly December to February (Figure 5). In the wet season, from June to November, the AET will be high in the SSP5-8.5 2050s GTW. Increasing the forestland contributes to increasing AET (Adane et al., 2018; Lv et al., 2019). In all climate scenarios and periods, the average monthly AET in the study area is expected to rise in comparison to the baseline. In the Ribb watershed, the average monthly AET is less than the Gumara. Without accounting for slope direction, the AET will decrease as the slope increases (Fu et al., 2025). Gumara AET's greater result might be attributed to the fact that its upper areas of the watershed are less rugged than Ribb's (Asfaw & Workineh, 2019).

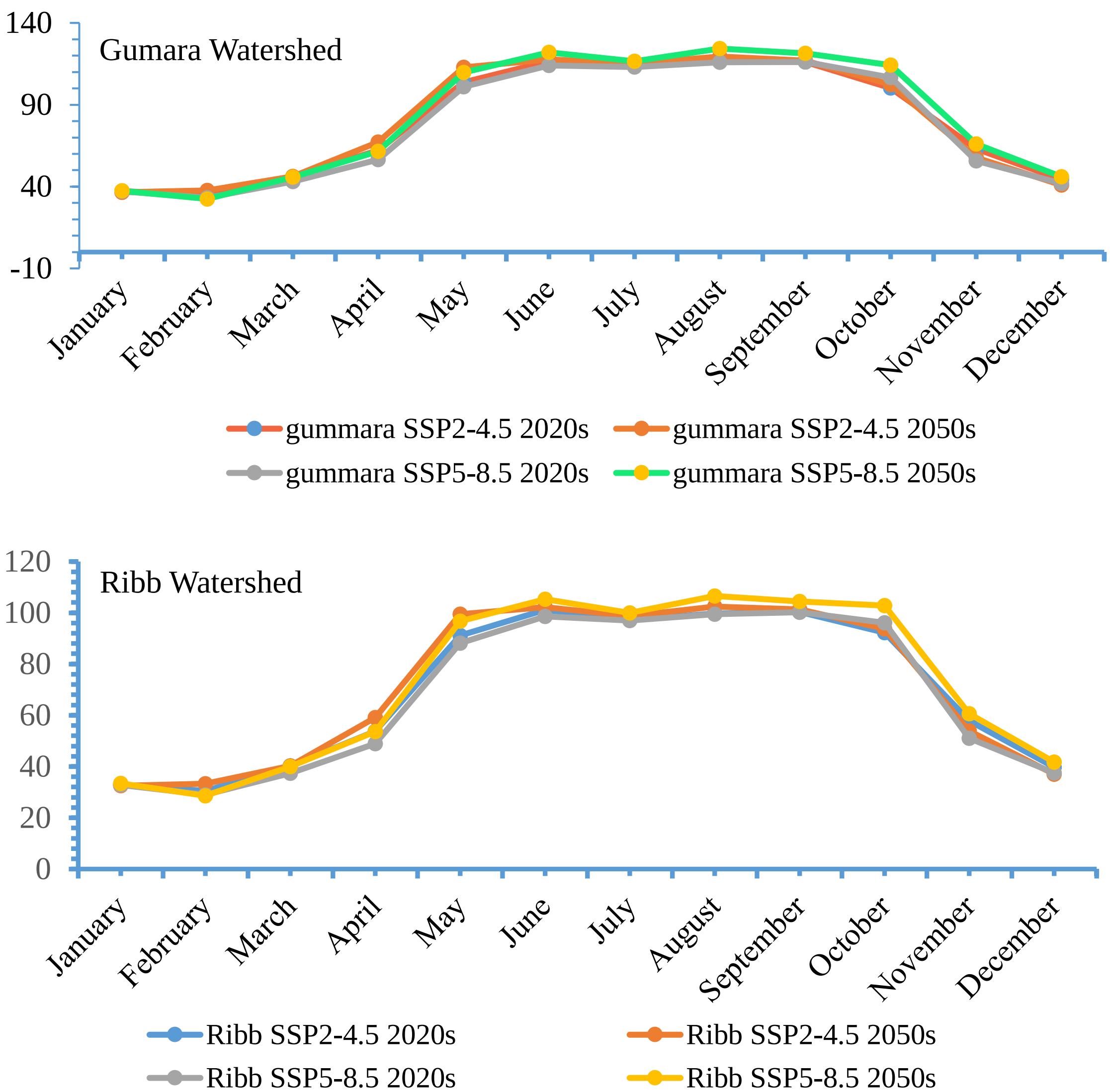

Figure 5. Average monthly AET in the two watersheds

3.6 Average seasonal changes of AET

The maximum seasonal change (33.5%) in SSP5-8.5 2050s was observed in Bega, or the dry season in Ethiopia, in the Ribb watershed. All seasons and scenarios are predicted to see significant rises in the Ribb watershed, with Bega exhibiting the most notable surge, especially under the high-emission SSP5-8.5 scenario in the 2050s, reaching over 30% above the baseline. Belg even indicates a modest fall under SSP5-8.5 in the 2020s, while the Gummar River shows more moderate changes, with minor increases in Kiremt and Bega. In general, the Gummar is quite stable, while the Ribb is more vulnerable to anticipated changes in the environment. The Ribb may experience increasingly significant seasonal water variability as a result of these trends, which emphasizes the necessity of adaptive water management techniques catered to watershed-specific reactions to climate change, as indicated in Table 4.

The watersheds may be harmed by the increase in AET, which results in decreased streamflow and groundwater recharge. Furthermore, the likelihood of drought is increased by soil moisture stress.

3.7. Annual change in AET

The projected changes in AET relative to the baseline period show distinct patterns between the Gumara and Ribb watersheds under different climate scenarios. In the Gumara watershed, AET is expected to increase moderately, by 3.25% in the 2020s and 1.19% in the 2050s under the SSP2-4.5 scenario. Under the more intensive SSP5-8.5 scenario, the increases are projected to reach 5.09% in the 2020s and 8.01% in the 2050s. The Ribb watershed, however, shows a more pronounced response. AET is projected to rise by 16.92% and 19.30% under SSP2-4.5 for the 2020s and 2050s, respectively, and by 14.13% and 22.07% under SSP5-8.5. These findings suggest that both watersheds will experience higher AET in the coming decades, with the Ribb watershed appearing more sensitive to future climate forcing.

The yearly average AET in both watersheds shows discernible increasing tendencies. The yearly AET in the Gelana watershed in Ethiopia is anticipated to rise in all forthcoming research periods under RCP4.5 and RCP8.5 up to 14.94% in 2071–2090 (Daniel & Abate, 2022). A comparable trend was perceived in the Gilgel Abay watershed, LTSB, Ethiopia, due to eucalypt trees replanting and an increase in agriculture (Ayele et al., 2018). The GTW has also increased eucalyptus plantations in the last decades may be a reason for to rise in AET. Annual AET revealed a positive increasing trend in Jemma, Ethiopia (Worku et al., 2021). Likewise, in all scenarios, the Awash basin experienced an increase in AET from 2.3 to 4.1% (Bekele et al., 2019). These studies are comparable to the GTW modeling result. The annual AET in the study watershed showed a mounting trend. The rise in vegetation tends to an upsurge in ET (Yu et al., 2021).

Table 4. Seasonal percentage change of AET

Watershed	Season	SSP2-4.5 2020s (%)	SSP2-4.5 2050s (%)	SSP5-8.5 2020s (%)	SSP5-8.5 2050s (%)
Ribb	Kiremt	11.85	13.53	10.77	16.74
	Bega	24.52	21.42	21.6	33.25
	Belg	20.13	29.04	13.1	21.83
Gumara	Kiremt	2.42	3.85	1.63	7.13
	Bega	6.26	3.13	4.66	14.44
	Belg	2.07	9.2	-3.16	3.27

4. Conclusions

Estimation of AET under LULC and climate alteration is vital to water balance, for effective planning and managing water resources for irrigation in agriculture. ENVI 5.3 was used for LULC detection, and the future land uses were predicted by QGIS 2.18.15 in the MOLUSCE plugin. This study examines the response of AET to LULC and climate change in the GTW, using streamflow-based calibrated MIKE SHE modeling software. The analysis was done for two periods (2020s and 2050s), considering SSP2-4.5 and SSP5-8.5. The projection of LULC is affected by population growth, economic expansion, and policy changes.

There were notable changes in the LULC from 1991 to 2049 that had a considerable effect on AET, jointly with climate change, in the watersheds. To reduce the uncertainty of GCM models ensemble of seven GCM outputs has been used to represent a reasonable range of outcomes. The baseline of climate models was 1985-2014, and the two periods of the 2020s (2016-2045) and the 2050s (2046-2075). In the GTW, the temperature is likely to rise, and a diminution of rainfall in most SSPs. The increase in temperature might cause to increase in AET. Reduction in rainfall and amplification in temperature have an impact on the production of agriculture, notably in arid and semi-arid contexts.

Mean annual AET relative to the baseline period indicates increasing trends in both the Gumara and Ribb watersheds under future climate scenarios. In the Gumara watershed, AET is expected to rise moderately, with increases of 3.25% and 1.19% in the 2020s and 2050s under SSP2-4.5, and 5.09% and 8.01% under SSP5-8.5. The Ribb watershed shows a stronger response, with AET increasing by 16.92% and 19.30% under SSP2-4.5, and 14.13% and 22.07% under SSP5-8.5.

Future minor alterations to AET will have varying effects on the watershed. This might limit GWR and streamflow, particularly during dry seasons. Increased water demand for irrigation is also a ramification of increased water demand for vegetation. The watershed's environment is impacted by the shift in AET. All of this presents problems for the environment and water balance downstream, such as Lake Tana. Future research should include additional climate models and ground truth data regarding plant characteristics, since this may increase model accuracy.

Acknowledgments:

The authors thank the Danish Hydraulic Institute (DHI), Denmark, for providing MIKE SHE/MIKE HYDRO software.

Author Contributions:

Damte Tegegne Fetene: Conceptualization, methodology, formal analysis and investigation, visualization, resources, writing-original draft preparation.

Tarun Kumar Lohani: Guidance, editing, and reviewing the article, controlling the results, supervision, and revision of the draft.

Abdella Kemal Mohammed: Methodology, formal analysis, and investigation, supervision.

Conflicts of interest

The authors of this article declared no conflict of interest regarding the authorship or publication of this article.

Data availability statement:

All data generated or analyzed during this study are included in this published article.

References

Abbasi, N., Nouri, H., Didan, K., Barreto-muñoz, A., Borujeni, S. C., Salemi, H., Opp, C., Siebert, S., & Nagler, P. (2021). Estimating Actual Evapotranspiration over Croplands Using Vegetation Index Methods and Dynamic Harvested Area. Remote Sensing, 13(5167). doi: 10.3390/rs13245167

Abdo, K. S., Fiseha, B. M., Rientjes, T. H. M., Gieske, A. S. M., & Haile, A. T. (2009). Assessment of climate change impacts on the hydrology of Gilgel Abay catchment in Lake Tana basin, Ethiopia. Hydrological Processes, 23(26), 3661–3669. doi: 10.1002/hyp

Abebe, S. A., Qin, T., Zhang, X., Li, C., & Yan, D. (2022). Estimating the Water Budget of the Upper Blue Nile River Basin with the Water and Energy Processes (WEP) Model. Frontiers in Earth Science, 10, 1–14. doi:10.3389/feart.2022.923252

Adane, Z. A., Nasta, P., Zlotnik, V., & Wedin, D. (2018). Impact of grassland conversion to forest on groundwater recharge in the Nebraska Sand Hills. Journal of Hydrology: Regional Studies, 15(June 2017), 171–183. doi: 10.1016/j.ejrh.2018.01.001

Addisu, S., Tadele, A., & Lema, H. (2024). Climate change and hydrological response of Megech catchment, Upper Blue Nile River Basin, Ethiopia. Geocarto International, 39(1). doi: 10.1080/10106049.2024.2335246

Addisuu, A. A., Tsidu, G. M., & Basupi, L. V. (2025). Improving Daily CMIP6 Precipitation in Southern Africa Through Bias Correction. Spatiotemporal Characteristics. Climate, 95(13), 1–38. doi: 10.3390/ cli13050095

Adjei, F. O., Obuobie, E., Adjei, K. A., & NOdai, S. (2023). Evaluation of potential evapotranspiration assessment methods for hydrological modelling with SWAT in the Densu River basin in Ghana. International Journal of Environmental Science and Technology, 20(1), 921–930. doi: 10.1007/s13762-022-03945-y

Afzal, M., & Ragab, R. (2020). Assessment of the potential impacts of climate change on the hydrology at catchment scale : modelling approach including prediction of future drought events using drought indices. Applied Water Science, 10(10), 1–19. doi: 10.1007/s13201-020-01293-1

Ahn, J., Baik, J., Kim, D., & Choi, M. (2018). A comparative assessment of SWAT-model-based evapotranspiration against regional-scale estimates. Ecological Engineering, 122(July), 1–9. doi: 10.1016/j.ecoleng.2018.07.015

Ajjur, S. B., & Al-Ghamdi, S. G. (2021). Evapotranspiration and water availability response to climate change in the Middle East and North Africa. Climatic Change, 167(3–4), 44. doi: 10.1007/s10584-021-03122-z

Al-Dousari, A. E., Mishra, A., & Singh, S. (2023). Land use land cover change detection and urban sprawl prediction for the Kuwait metropolitan region, using multi-layer perceptron neural networks (MLPNN). Egyptian Journal of Remote Sensing and Space Science, 26(2), 381–392. doi: 10.1016/j.ejrs.2023.05.003

Alebachew, S., Tesfahun, A., & Kebtieneh, N. (2022). Abundance, distribution, and diversity of fishes in Ribb Reservoir, Lake Tana basin, Ethiopia. Cogent Food & Agriculture, 8(1). doi: 10.1080/23311932.2022.2105934

Alemu, M. L., Worqlul, A. W., Zimale, F. A., Tilahun, S. A., & Steenhuis, T. S. (2020). Water Balance for a Tropical Lake in the Volcanic Highlands: Lake Tana, Ethiopia. Water. doi: 10.3390/w12102737

Amare, M. T., Demissie, S. T., Beza, S. A., & Erena, S. H. (2023). Land Cover Change Detection and Prediction in the Fafan Catchment of Ethiopia. Journal of Geovisualization and Spatial Analysis, 7(2), 1–11. doi: 10.1007/s41651-023-00148-y

Amgoth, A., Ponnamma, H., & Jayakumar, R. K. V. (2023). Exploring LULC changes in Pakhal Lake area, Telangana, India, using QGIS MOLUSCE plugin. Spatial Information Research, 1–10. doi: 10.1007/s41324-023-00509-1

Asfaw, D., & Workineh, G. (2019). Quantitative analysis of morphometry on Ribb and Gumara watersheds: Implications for soil and water conservation. International Soil and Water Conservation Research, 7(2), 150–157. doi: 10.1016/j.iswcr.2019.02.003

Awada, H., Di Prima, S., Sirca, C., Giadrossich, F., Marras, S., Spano, D., & Pirastru, M. (2021). Daily actual evapotranspiration estimation in a Mediterranean ecosystem from Landsat observations using SEBAL approach. Forests, 12(2), 1–20. doi: 10.3390/f12020189

Ayalew, S. E., Niguse, T. A., & Aragaw, H. M. (2024). Hydrological responses to historical and predicted land use/land cover changes in the Welmel watershed, Genale Dawa Basin, Ethiopia : Implications for water resource management. Journal of Hydrology: Regional Studies, 52(October 2023), 101709. doi: 10.1016/j.ejrh.2024.101709

Ayele, H. S., Li, M.-H., Tung, C.-P., & Liu, T.-M. (2016). Impact of Climate Change on Runoff in the Gilgel Abbay Watershed, the Upper Blue Nile Basin, Ethiopia. Water (Switzerland), 8(380). doi: 10.3390/w8090380

Ayele, T., Ahmed, N., Ribbe, L., & Heinrich, J. (2018). Catchment response to climate and land use changes in the Upper Blue. Science of the Total Environment, 644, 193–206. doi: 10.1016/j.scitotenv.2018.06.198

Bekele, A. A., Pingale, S. M., Hatiye, S. D., & Tilahun, A. K. (2019). Impact of climate change on surface water availability and crop water demand for the sub-watershed of Abay Basin, Ethiopia. Sustainable Water Resources Management, 2016. doi: 10.1007/s40899-019-00339-w

Bekele, D., Alamirew, T., Kebede, A., Zeleke, G., & M. Melesse, A. (2019). Modeling Climate Change Impact on the Hydrology of Keleta Watershed in the Awash River Basin, Ethiopia. Environmental Modeling and Assessment, 24(1), 95–107. doi: 10.1007/s10666-018-9619-1

Belay, T., Melese, T., & Senamaw, A. (2022). Impacts of land use and land cover change on ecosystem service values in the Afroalpine area of Guna Mountain, Northwest Ethiopia.

Heliyon, 8(12), e12246 doi: 10.1016/j.heliyon.2022.e12246

Berhanu, K. G., Lohani, T. K., & Hatiye, S. D. (2024). Long-term spatiotemporal dynamics of groundwater storage in the data-scarce region: Tana sub-basin, Ethiopia. Heliyon, 10(3), e24474. doi: 10.1016/j.heliyon.2024.e24474

Beyene, A., Cornelis, W., Verhoest, N. E. C., Tilahun, S., Alamirew, T., Adgo, E., De Pue, J., & Nyssen, J. (2018). Estimating the actual evapotranspiration and deep percolation in irrigated soils of a tropical floodplain, northwest Ethiopia. Agricultural Water Management, 202(June 2017), 42–56. doi: 10.1016/j.agwat.2018.01.022

Birhanu, D., & Kim, H. (2019). Effectiveness of introducing crop coefficient and leaf area index to enhance evapotranspiration simulations in hydrologic models. Hydrological Processes, 2206–2226. doi: 10.1002/hyp.13464

Cao, X., Zheng, Y., Lei, Q., Li, W., Song, S., & Wang, C. (2023). Increasing actual evapotranspiration on the Loess Plateau of China : An insight from anthropogenic activities and climate change. Ecological Indicators, 157, 111235.doi: 10.1016/j.ecolind.2023.111235

Chen, C., Kalra, A., & Ahmad, S. (2018). Hydrologic responses to climate change using downscaled GCM data on a watershed scale. Journal of Water and Climate Change, 147, 1–15. doi: 10.2166/wcc.2018.147

Chen, M., Samat, N., Maghsoodi Tilaki, M. J., & Duan, L. (2025). Land use/cover change simulation research: A system literature review based on bibliometric analyses. Ecological Indicators,.doi: 10.1016/j.ecolind.2025.112991

Chen, Z., Nong, X., Zang, C., Ou, W., & Qiu, L. (2024). Evolution of evapotranspiration in the context of land cover/climate change in the Han River catchment of China. Hydrological Processes, 38(8). doi: 10.1002/hyp.15265

Daniel, H., & Abate, B. (2022). Effect of climate change on streamflow in the Gelana watershed, Rift Valley basin, Ethiopia. Journal of Water and Climate Change, 13(5), 2205–2232. doi: 10.2166/wcc.2022.059

Das, J., Poonia, V., Jha, S., & Goyal, M. K. (2020). Understanding the climate change impact on crop yield over the Eastern Himalayan Region : ascertaining GCM and scenario uncertainty. Theoretical and Applied Climatology, 142, 467–482. doi: 10.1007/s00704-020-03332-y

Deb, P., Babel, M. S., & Francis, A. (2018). Multi-GCMs approach for assessing climate change impact on water resources in Thailand. Modeling Earth Systems and Environment, 4(2), 825–839. doi: 10.1007/s40808-018-0428-y

Demirel, M. C., Mai, J., Mendiguren, G., Koch, J., Samaniego, L., & Stisen, S. (2018). Combining satellite data and appropriate objective functions for improved spatial pattern performance of a distributed hydrologic model. Hydro.Earth System Science, 22, 1299–1315. doi: 10.5194/hess-22-1299-2018

Doost, Z. H., & Yaseen, Z. M. (2025). The impact of land use and land cover on groundwater fluctuations using remote sensing and geographical information systems : Representative case study in Afghanistan. Environment, Development and Sustainability, 27(4), 9515–9538. doi: 10.1007/s10668-023-04253-2

Duan, Q., Pappenberger, F., Wood, A., Cloke, H. L., & Schaake, J. C. (2019). Handbook of Hydrometeorological Ensemble Forecasting. doi: 10.1007/978-3-642-39925-1

Dufera, T., & Brijesh, T. (2023). Assessment of land use/land cover change impact on streamflow: a case study over Upper Guder Catchment, Ethiopia. Sustainable Water Resources Management, 9(1), 1–12. doi: 10.1007/s40899-022-00783-1

Farjad, B., Gupta, A., Razavi, S., Faramarzi, M., & Marceau, D. J. (2017). An integrated modelling system to predict hydrological processes under climate and land-use/cover change scenarios. Water, 9(10), 767. doi: 10.3390/w9100767

Ferede, M., Gedle, A., Yimer, A. K., & Amare, S. D. (2022). Implications of Uncontrolled Water Withdrawal and Climate Change on Water Supply and Demand Gap in Tana Lake Sub-basin. Ethiopian Journal of Water Science and Technology (EJWST), 5, 74–101. doi: 10.59122/15519a9

Fetene, D. T., Kumar, T. L., & Mohammed, A. K. (2023). LULC change detection using support vector machines and cellular automata-based ANN models in Guna Tana watershed of Abay basin, Ethiopia. Environmental Monitoring and Assessment, 195(1329). doi: 10.1007/s10661-023-11968-2

Fetene, D. T., Lohani, T. K., & Mohammed, A. K. (2024). Application of coupled MIKE SHE / MIKE HYDRO on streamflow dynamics under climate change in Lake Tana sub-basin, Abay Basin, World Water Policy, and June 1–24. doi: 10.1002/wwp2.12225

Fu, W., Tang, B., Member, S., Ma, X., Zhu, X., Li, Y., & Cheng, L. (2025). Assessing Terrain Effect on Evapotranspiration Using the SEBAL Model in Mountainous Regions. IEEE Journal of Selected Topics in Applied Earth Observations and Remote Sensing, 18, 6017–6040. doi: 10.1109/JSTARS.2025.3539822

Ganguli, A., Feinstein, J., Raji, I., Akinsanola, A., Aghili, C., Jung, C., Branham, J., Wall, T., Huang, W., & Kotamarthi, R. (2025). Bias Correcting Regional Scale Earth Systems Model Projections : Novel Approach using Empirical Mode Decomposition. Egusphere.Copernicus, March. doi: Bias correcting Regional Scale Earth Systems Model Projections: Novel Approach.doi: 10.5194/egusphere-2025-1112

Gao, W., Wang, Z., & Huang, G. (2020). Spatiotemporal Variability of Actual Evapotranspiration and the Dominant Climatic Factors in the Pearl River Basin, China. Atmosphere. doi: 10.3390/atmos10060340

Getachew, B., & Manjunatha, B. R. (2021). Climate change projections and trends simulated from the CMIP5 models for the Lake Tana sub-basin, the Upper Blue Nile (Abay) River Basin, Ethiopia. Environmental Challenges, 5(November), 1–22. doi: 10.1016/j.envc.2021.100385

Ghaderi, A., Dasineh, M., Shokri, M., & Abraham, J. (2020). Estimation of actual evapotranspiration using the remote sensing method and SEBAL algorithm: A case study in Ein Khosh Plain, Iran. Hydrology, 7(36). doi: 10.3390/hydrology7020036

Gisolo, D., Previati, M., Bevilacqua, I., Canone, D., Boetti, M., Dematteis, N., & Balocco, J. (2022). A calibration-free radiation-driven model for estimating actual evapotranspiration of mountain grasslands (CLIME-MG). Journal of Hydrology, 610(November 2021), 127948. doi: 10.1016/j.jhydrol.2022.127948

Gholami, H., Lotfirad, M., Ashrafi, S. M., Biazar, S. M., & Singh, V. P. (2023). Multi-GCM ensemble model for reduction of uncertainty in runoff projections. Stochastic Environmental Research and Risk Assessment, 37(4), 953–964. doi: 10.1007/s00477-022-02311-1

Granata, F. (2019). Evapotranspiration evaluation models based on machine learning algorithms—a comparative study. Agricultural Water Management, 217(January), 303–315. doi: 10.1016/j.agwat.2019.03.015

Hejia, W., Weihua, X., Zhao, Y., Wang, Y., Hou, B., Zhou, Y., Yang, H., Zhang, X., & Cui, H. (2019). The spatiotemporal variability of evapotranspiration and its response to climate change and land use/land cover change in the Three Gorges Reservoir. Water (Switzerland), 11(9). doi: 10.3390/w11091739

Hong, S., Deng, H., Zheng, Z., & Deng, Y. (2023). The influence of variations in actual evapotranspiration on drought in China's Southeast River basin. Scientific Reports, 13, 1–13. doi: 10.1038/s41598-023-48663-8.

Hyandye, C.B., Worqul, A., Martz, L.W. & Muzuka, A.N.N., 2018. The impact of future climate and land use/cover change on water resources in the Ndembera watershed and their mitigation and adaptation strategies. Environmental Systems Research, 7, Article 7. Doi: 10.1186/s40068-018-0110-4.

Ji, Z., Wang, Y., & Wang, L. (2024). Threshold identification of evapotranspiration under different land-use types in the Loess Plateau, China. Journal of Hydrology: Regional Studies, 53(April), 101780. doi: 10.1016/j.ejrh.2024.101780.

Kim, T. (2024). Projected changes in daily precipitation, temperature, and wet-bulb temperature across Arizona using statistically downscaled CMIP6 climate models. International Journal of Climatology, October 2023, 1994–2010. doi: 10.1002/joc.8436

Kindie, A., Enku, T., Moges, M. A., Geremew, B. S., & Atinkut, H. B. (2019). Spatial Analysis of Groundwater Potential Using GIS-Based Multi-Criteria Decision Analysis Method in Lake Tana Basin, Ethiopia. In Springer Nature (Vol. 274, pp. 439–456). doi: 10.1007/978-3-030-15357-1

Kuma, H. G., Feyessa, F. F., & Demissie, T. A. (2021). Hydrologic responses to climate and land-use / land-cover changes in the Bilate catchment, Southern Ethiopia. Journal of Water and Climate Change, 12(8), 3750–3769. doi: 10.2166/wcc.2021.281

Kundu, S., Mondal, A., Khare, D., Hain, C., & Lakshmi, V. (2018). Projecting climate and land use change impacts on actual evapotranspiration for the Narmada river basin in Central India in the future. Remote Sensing, 10(4), 1–22. doi: 10.3390/rs10040578

Lanfredi, M., Coluzzi, R., & Imbrenda, V. (2022). Editorial for the Special Issue "Advances of Remote Sensing in the Analysis of the Spatial and Temporal Variability of Land Surface." Remote Sensing. doi: 10.3390/rs14236123

Lee, S. K., Dang, T. A., & Tran, T. H. (2018). Combining rainfall–runoff and hydrodynamic models for simulating flow under the impact of climate change on the lower Sai Gon-Dong Nai River basin. Paddy and Water Environment, 16(3), 457–465. doi: 10.1007/s10333-018-0639-x

Li, X., Pang, Z., Xue, F., Ding, J., Wang, J., Xu, T., Xu, Z., & Ma, Y. (2024). Analysis of Spatial and Temporal Variations in Evapotranspiration and Its Driving Factors Based on Multi-Source Remote Sensing Data : A Case Study of the Heihe River Basin. Remote Sensing, 1–25. doi: 10.3390/rs16152696

Li, Y., Cai, Y., Wang, X., Li, C., Liu, Q., Sun, L., & Fu, Q. (2022). Classification of Blue Water and Green Water: A Case Study in the Yalong River Basin, Southwest China. Journal of Environmental Management. doi: 10.1016/j.jenvman.2022.115894

Liyew, M., Tsunekawa, A., Haregeweyn, N., Berihuna, M. L. A. T., Haregewey, N., Derege Tsegaye Mesheshae, E. A., Tsuboc, M., Masunagaf, T., Ayele Almaw Fentac, D. S., & Yibeltal, M. (2019). Land Use Policy: Exploring land use/land cover changes, drivers, and their implications in contrasting agro-ecological environments of Ethiopia. Land Use Policy, 87(June), 104052. doi: 10.1016/j.landusepol.2019.104052

Lu, Z., Li, C., Zhang, J., Lei, G., Yu, Z., & Dong, Z. (2024). Impact of land use change on actual evapotranspiration in the Songnen Plain, China. Journal of Hydrology: Regional Studies, 54, 101854. doi: 10.1016/j.ejrh.2024.101854

Lu, Z., Zhang, J., Li, C., Wang, X., Lei, G., & Li, K. (2025). Modeling hydrological processes and analyzing water balance utilizing remote sensing data and physical hydrological models in the Songnen Plain, China. PLoS ONE. doi: 10.1371/journal.pone.0329816

Lv, X., Zuo, Z., Sun, J., Ni, Y., & Wang, Z. (2019). Climatic and human-related indicators and their implications for evapotranspiration management in a watershed of the Loess Plateau, China. Ecological Indicators, 101(January), 143–149. doi: 10.1016/j.ecolind.2019.01.019

Ma, N., & Szilagyi, J. (2019). The CR of Evaporation: A Calibration-Free Diagnostic and Benchmarking Tool for Large-Scale Terrestrial Evapotranspiration Modeling. Water Resources Research, 7246–7274. doi: 10.1029/2019WR024867

Marek, G. W., Gowda, P. H., Evett, S. R., Baumhardt, R. L., Brauer, D. K., Howell, T. A., Marek, T. H., & Srinivasan, R. (2016). Estimating Evapotranspiration for Dryland Cropping Systems in the Semiarid Texas High Plains Using SWAT. Journal of the American Water Resources Association, 52(2). doi: 10.1111/1752-1688.12383

Mebrie, D. W., Assefa, T. T., Yimam, A. Y., & Belay, S. A. (2023). A remote sensing approach to estimate variable crop coefficient and evapotranspiration for improved water productivity in the Ethiopian highlands. Applied Water Science, 13(8), 1–15. doi: 10.1007/s13201-023-01968-5

Mekonnen, K., M.Melesseb, A., & Woldesenbet, T. A. (2021). How suitable are satellite rainfall estimates in simulating high flows and actual evapotranspiration in the MelkaKunitre catchment, Upper Awash Basin, Ethiopia?

Science of the Total Environment. doi: 10.1016/j.scitotenv.2021.150443

Moges, D. M., & Bhat, H. G. (2017). Integration of geospatial technologies with RUSLE for analysis of land use/cover change impact on soil erosion: case study in Rib watershed, northwestern highland, Ethiopia. Environmental Earth Sciences, 76(22). doi: 10.1007/s12665-017-7109-4

Mohamed, A., Werner, M., & Zaag, P. van der. (2025). Beyond streamflow: Plausible hydrological modelling for the Upper Blue Nile Basin, Ethiopia. Journal of Hydrology: Regional Studies, 59, 102290. doi: 10.1016/j.ejrh.2025.102290

Mulatu, C. A., Crosato, A., Langendoen, E. J., Michael, M., & McClain, M. E. (2021). Alteration of the Fogera Plain flood regime due to Ribb Dam construction, Upper Blue Nile Basin, Ethiopia. Journal of Applied Water Engineering and Research,doi: 10.1080/23249676.2021.1961618

Nannawo, A. S., Lohani, T. K., & Eshete, A. A. (2022). Envisaging the actual evapotranspiration and elucidating its effects under climate change scenarios on the agrarian lands of the Bilate River basin in Ethiopia. Heliyon, 8(August), e10368. doi: 10.1016/j.heliyon.2022.e10368

Nunno, F. Di, & Granata, F. (2023). Future trends of reference evapotranspiration in Sicily based on CORDEX data and Machine Learning algorithms. Agricultural Water Management, 280 108232.doi: 10.1016/j.agwat.2023.108232

Omondi, V., Richard, P., Oel, V., Tol, C. Van Der, & Su, Z. (2019). Impact of land use and land cover transitions and climate on evapotranspiration in the Lake Naivasha Basin, Kenya. Science of the Total Environment, 682, 19–30. doi: 10.1016/j.scitotenv.2019.04.062

Pan, S., Liu, L., Bai, Z., & Xu, Y. (2018). Integration of Remote Sensing Evapotranspiration into Multi-Objective Calibration of Distributed Hydrology–Soil–Vegetation Model (DHSVM) in a Humid Region of China. Water (Switzerland), 10(1841), 1–18. doi: 10.3390/w10121841

Patel, V. D. L. and P. L. (2018). Performance evaluation and parameter sensitivity of a distributed hydrological model for a semi-arid catchment in India. Journal of Earth System Science, 11(September), 122–133. doi: 10.5897/JGRP2018.0707

Peng, L., Wei, Z., Chen, A., Wood, E. F., & Sheffield, J. (2019). Determinants of the ratio of actual to potential evapotranspiration. Global Change Biology, January, 1326–1343. doi: 10.1111/gcb.14577

Puttinaovarat, S., Khaimook, K., & Horkaew, P. (2025). Land use and land cover classification from satellite images based on ensemble machine learning and crowdsourced data verification. International Journal of Cartography, 11(1), 3–23.doi: 10.1080/23729333.2023.2166252.

Qilin, W., Cheng, L., Zhang, L., Liu, P., Qin, S., Liu, L., & Jing, Z. (2021). Quantifying the impacts of land-cover changes on global evapotranspiration based on the continuous remote sensing observations during 1982–2016. Journal of Hydrology, 598(February), 126231. doi: 10.1016/j.jhydrol.2021.126231

Rahim, B. E. A., & Yusoff, I. (2023). A practical approach for numerical modeling of a complex and data-limited hydrological system. Hydrology Research, 54(11). doi: 10.2166/nh.2023.048

Rahim, B. E. A., Yusoff, I., Jafri, A. M., Othman, Z., & Abdul Ghani, A. (2012). Application of the MIKE SHE modelling system to set up a detailed water balance computation. Water and Environment Journal, 26(4). doi: 10.1111/j.1747-6593.2012.00309.x

Rahman, F., & Rahman, M. T. U. (2023). Use of cellular automata-based artificial neural networks for detection and prediction of land use changes in North-Western Dhaka City. Environmental Science and Pollution Research. doi: 10.1007/s11356-022-22079-9.

Savaresi, A. (2016). The Paris Agreement : a new beginning ? Journal of Energy & Natural Resources Law, 6811(34), 16–26. doi: 10.1080/02646811.2016.1133983

Seifu, T. K., & Eshetu, K. D. (2024). Characterizing the aridity indices and potential evapotranspiration using CMIP6-GCMs in two distinct regions of Ethiopia. Journal of Water and Climate Change, 15(4), 1507–1531. doi: 10.2166/wcc.2024.394

Senay, G. B., Kagone, S., & Velpuri, N. M. (2020). Operational global actual evapotranspiration: Development, evaluation, and dissemination. Sensors (Switzerland), 20(7), 1–18. doi: 10.3390/s20071915

Seo, S. B., Kim, Y., Kim, Y., & Eum, H. (2019). Selecting climate change scenarios for regional hydrologic impact studies based on climate extremes indices. Climate Dynamics, 52(3), 1595–1611. doi: 10.1007/s00382-018-4210-7

Setegn, S. G., Srinivasan, R., & Dargahi, B. (2008). Hydrological Modelling in the Lake Tana Basin, Ethiopia Using the SWAT Model. The Open Hydrology Journal, 49–62

Sharma, A., Kumar, A., Shankar, V., & Thakur, P. K. (2024). Hydrological modeling for rainfall–runoff assessment in a sub-himalayan catchment using a distributed MIKE SHE/MIKE+ model. Water Practice and Technology, 00(1), 1–15. doi: 10.2166/wpt.2024.158

Shen, M., Chen, J., Zhuan, M., Chen, H., Xu, C. Y., & Xiong, L. (2018). Estimating uncertainty and its temporal variation related to global climate models in quantifying climate change impacts on hydrology. Journal of Hydrology, 556, 10–24. doi: 10.1016/j.jhydrol.2017.11.004

Shing, S., Karlsson, I., & Karsten, H. (2021). Climate change impacts and uncertainty on spatiotemporal variations of drought indices for an irrigated catchment. Journal of Hydrology, 601(August).doi: 10.1016/j.jhydrol.2021.126814.

Shiru, M. S., Kim, J. H., & Chung, E.-S. (2022). Variations in projections of precipitation of CMIP6 global climate models under SSP 2-4.5 and SSP 5-8.5. KSCE Journal of Civil Engineering, 26(12), 5404–5416. doi: 10.1007/s12205-022-0149-7

Siabi, E. K., Awafo, E. A., Kabo-bah, A. T., Sarfo, N., Derkyi, A., Akpoti, K., Mortey, E. M., & Yazdanie, M. (2023). Assessment of Shared Socioeconomic Pathway (SSP) climate scenarios and their impacts on the Greater Accra region. Urban Climate, 49. doi: 10.1016/j.uclim.2023.101432

Sinha, M. K., Rajput, P., Baier, K., & Azzam, R. (2021). GIS-Based Assessment of Urban Groundwater Pollution Potential Using Water Quality Indices. Springer Nature Switzerland. doi: 10.1007/978-3-030-68124-1_15

Soumya, P., & Neeta, K. (2023). Prediction and monitoring of LULC shift using cellular automata-artificial neural network in Jumar watershed of Ranchi District, Jharkhand. Environmental Monitoring and Assessment, 195(1). doi: 10.1007/s10661-022-10623-6

Tarafdar, A., Iqbal, A., Sounak, M., & Sunirmal, B. (2025). A CNN-based framework for land use and land cover classification of heterogeneous terrain using satellite images. Neural Computing and Applications, 37(21), 16381–16408. doi: 10.1007/s00521-025-11314-2

Taye, M. T., Haile, A. T., Fekadu, A. G., & Nakawuka, P. (2021). Effect of irrigation water withdrawal on the hydrology of the Lake Tana sub-basin. Journal of Hydrology: Regional Studies, 38(November), 100961. doi: 10.1016/j.ejrh.2021.100961

Teressa, H., Minale, H., Birie, S., & Alemayehu, Y. (2021). Marginalized groups of Gelada (Theropithecus gelada) living in and around the highly disturbed Mount Guna Community Conservation Area, Northwest Ethiopia. International Journal of Ecology, 2021, 6673622. doi: 10.1155/2021/6673622

Tikuye, B. G., Ray, R. L., Gebeyehu, K., & Teshome, M. (2024). Assessing the influence of land use/land cover dynamics and climate change on water resources in Upper Blue Nile, Ethiopia. Journal of Water and Climate Change, 15(9), 4745–4774. doi: 10.2166/wcc.2024.319

Vu, M. T., VO, N. D., P., G., S.V., R., & Liong, S.-Y. (2017). Hydro-meteorological drought assessment under climate change impact over the Vu Gia–Thu Bon River basin, Vietnam. Hydrological Sciences Journal, June, 1–28. doi: 10.1080/02626667.2017.1346374

Wang, B., Li, S., & Ge, Y. (2023). Numerical Simulation of the Lower and Middle Reaches of the Yarkant River (China) Using MIKE SHE. Water (Switzerland), 15, 1–19. doi: 10.3390/w15132492

Werede, K. Z., Lohani, T. K., Neka, B. G., & Geremew, G. B. (2024). Modeling streamflow responses to land use and land cover change using the MIKE SHE model in the upper Omo

Gibe catchment of Ethiopia. World Water Policy. doi: 10.1002/wwp2.12186

Worku, G., Teferi, E., Bantider, A., & Dile, Y. T. (2021). Modelling hydrological processes under climate change scenarios in the Jemma sub-basin of Upper Blue Nile Basin, Ethiopia. Climate Risk Management, 31(July 2020), 100272. doi: 10.1016/j.crm.2021.100272

Worqlul, A. W., Taddele, Y. D., Ayana, E. K., Jeong, J., Adem, A. A., & Gerik, T. (2018). Impact of climate change on streamflow hydrology in headwater catchments of the upper Blue Nile Basin, Ethiopia. Water, 10(2). doi: 10.3390/w10020120

Wu, C., Hu, B. X., Huang, G., & Zhang, H. (2017). Effects of climate and terrestrial storage on temporal variability of actual evapotranspiration Effects of climate and terrestrial storage on temporal variability of actual evapotranspiration. Journal of Hydrology, 549(April), 388–403. doi: 10.1016/j.jhydrol.2017.04.012

Wu, H., Yang, C., Xie, C., Man, Z., He, S., Qin, Y., & Che, S. (2024). Quantification of the contribution of climate change and land use change on urban ecosystem service using a multi-scale approach. Ecological Indicators, 167(September), 112619. doi: 10.1016/j.ecolind.2024.112619

Wu, X., Liu, Z., & Duan, Q. (2023). A combined wavelet analysis-quantile mapping (WA-QM) method for bias correction: capturing the intra-annual temporal patterns in climate model precipitation simulations and projections. Environmental Research Letters, 20. doi: 10.1088/1748-9326/adae23

Wubneh, M. A., Worku, T. A., Fikadie, F. T., Aman, T. F., & Alemu, M. G. (2024). Operational analysis of Lake Tana under climate change, Upper Blue Nile Basin, Ethiopia. Scientific African,24.doi: 10.1016/j.sciaf.2024.e02217

Xiong, M., Liu, P., Cheng, L., Deng, C., Gui, Z., & Zhang, X. (2019). Identifying time-varying hydrological model parameters to improve simulation efficiency by the ensemble Kalman filter: A joint assimilation of streamflow and actual evapotranspiration. Journal of Hydrology, 568(December 2017), 758–768. doi: 10.1016/j.jhydrol.2018.11.038

Yang, J., Wang, W., Hua, T., & Peng, M. (2020). Spatiotemporal variation of actual evapotranspiration and its response to change of major meteorological factors over China using multi-source data. Journal of Water and Climate Change. doi: 10.2166/wcc.2020.221

Yang, L., Feng, Q., Li, C., Si, J., Wen, X., & Yin, Z. (2017). Detecting climate variability impacts on reference and actual evapotranspiration in the Taohe River Basin, China. Hydrology Research, 48(2) 596–612. doi: 10.2166/nh.2016.252

Yu, Y., Zhou, Y., Xiao, W., Ruan, B., Lu, F., Hou, B., Wang, Y., & Cui, H. (2021). Impacts of climate and vegetation on actual evapotranspiration in typical arid mountainous regions using a Budyko-based framework. Hydrology Research, 52(1), 212–228. doi: 10.2166/nh.2020.051

Yuning, L., Zhang, K., Wang, W., Chen, X., & Jin, F. (2025). An improved statistical bias correction method for Global Climate Model (GCM) precipitation projection: A case study on the CMCC-CM2-SR5 model projection in China's Huaihe River Basin. Journal of Hydrology and Regional Studies, 57, 1–23. doi: 10.1016/j.ejrh.2024.102146

Zhang, Q., Yang, Z., Hao, X., & Yue, P. (2019). Conversion features of evapotranspiration responding to climate warming in transitional climate regions in northern China. Climate Dynamics, 52(7), 3891–3903. doi: 10.1007/s00382-018-4364-3

Zheng, Q., Hao, L., Huang, X., Sun, L., & Sun, G. (2020). Effects of urbanization on watershed evapotranspiration and its components in southern China. Water (Switzerland), 12(3). doi: 10.3390/w12030645